

The quantum future of microscopy: Wave function engineering of electrons, ions, and nuclei

Cite as: Appl. Phys. Lett. **116**, 230502 (2020); <https://doi.org/10.1063/1.5143008>

Submitted: 19 December 2019 . Accepted: 29 May 2020 . Published Online: 11 June 2020

I. Madan , G. M. Vanacore, S. Gargiulo, T. LaGrange, and F. Carbone 



View Online



Export Citation



CrossMark

ARTICLES YOU MAY BE INTERESTED IN

[Superconducting quantum many-body circuits for quantum simulation and computing](#)

Applied Physics Letters **116**, 230501 (2020); <https://doi.org/10.1063/5.0008202>

[How many photons does it take to form an image?](#)

Applied Physics Letters **116**, 260504 (2020); <https://doi.org/10.1063/5.0009493>

[Developing silicon carbide for quantum spintronics](#)

Applied Physics Letters **116**, 190501 (2020); <https://doi.org/10.1063/5.0004454>



Your Qubits. Measured.

Meet the next generation of quantum analyzers

- Readout for up to 64 qubits
- Operation at up to 8.5 GHz, mixer-calibration-free
- Signal optimization with minimal latency

Find out more



The quantum future of microscopy: Wave function engineering of electrons, ions, and nuclei

Cite as: Appl. Phys. Lett. **116**, 230502 (2020); doi: [10.1063/1.5143008](https://doi.org/10.1063/1.5143008)

Submitted: 19 December 2019 · Accepted: 29 May 2020 ·

Published Online: 11 June 2020



View Online



Export Citation



CrossMark

I. Madan,  G. M. Vanacore, S. Gargiulo, T. LaGrange, and F. Carbone^{a)} 

AFFILIATIONS

Laboratory for Ultrafast Microscopy and Electron Scattering (LUMES), Institute of Physics (IPhys), Ecole Polytechnique Federale de Lausanne (EPFL), Lausanne 1015 CH, Switzerland

^{a)} Author to whom correspondence should be addressed: fabrizio.carbone@epfl.ch

ABSTRACT

The ability to manipulate particles has always been a fundamental aspect for developing and improving scattering and microscopy techniques used for material investigations. So far, microscopy applications have mostly relied on a classical treatment of the electron-matter interaction. However, exploiting a particle's quantum nature can reveal novel information not accessible with conventional schemes. Here, after describing recent methods for coherent wave function engineering, we discuss how quantum manipulation of electrons, He ions, and nuclei can be used to implement low-dose imaging methods, to explore correlated quantum state dynamics in condensed matter, and to modulate nuclear reactions for energy-related applications and gamma-ray lasers.

© 2020 Author(s). All article content, except where otherwise noted, is licensed under a Creative Commons Attribution (CC BY) license (<http://creativecommons.org/licenses/by/4.0/>). <https://doi.org/10.1063/1.5143008>

Transmission electron microscopy (TEM) established itself as a versatile technique for material science,¹ optoelectronics,² condensed matter,³ and biophysics.⁴ In this broad scope of disciplines, TEM techniques have been used predominantly to extract classical or semi-classical information about the samples—atomic positions, sample orientation, morphology, and composition, together with the spatial distribution of excitations via energy-filtered TEM or cathodoluminescence. In recent years, new methods exploiting the quantum nature of electrons emerged, offering interesting developments of TEM techniques, as well as some unexpected perspectives. In this Letter, we comment on new methods that we find particularly fascinating and propose a few potentially disruptive applications.

The quantum mechanical approaches to electron microscopy can be subjectively divided into three broad categories: (1) experiments based on interference effects, (2) experiments based on the longitudinal-phase modulation of the electron wave function, and (3) experiments based on the transverse-phase modification of the electron wave function. In the first half of this perspective, we illustrate experiments from each category and theorize on future applications. In the second half, we consider how the concepts emerged from TEM experiments can be applied beyond conventional electron microscopy, with a particular focus on beams of composite particles, such as neutrons, protons, and atomic nuclei.

In the first topic, we discuss the latest concerted efforts in implementing interaction-free measurements for dose reduction

experiments. This concept was envisioned primarily in the context of imaging the three-dimensional (3D) structure of biological molecules in close-to-natural environments without extensive sample preparation that can perturb molecular structures, for which TEM has been revolutionarily useful in the latest years.⁵ In particular, the development of cryo-EM has allowed scientists to address individual proteins in aqueous surroundings,^{6,7} defining our understanding of how geometry affects biological functions and allowing a deep understanding of how our body works on the molecular level.⁸ Conceptually, the next big leap would be an observation of the real-time dynamics of molecules in their biological processes.^{9–11} In condensed matter and material science, such advances already emerged, in which observing in direct space and real-time atomic motions,^{9,12} charge,¹³ and spin dynamics¹⁴ are a reality. The main obstacle for biological imaging, even in static observations, is radiation damage. As molecules comprise very light atoms that are not confined in a rigid crystalline structure, they can sustain small irradiating electron doses.¹⁵ Overcoming this limitation has been inspirational for new approaches, with new experimental,^{16–18} instrumental,^{19–22} computational,^{23–26} and conceptual^{27,28} schemes proposed.

A particularly interesting and disruptive concept in this context is the so-called *interaction-free* measurement, often referred to as the quantum electron microscope, which takes advantage of the quantum nature of electrons.²⁹ This approach is based on the Elitzur–Vaidman³⁰ thought experiment, which hypothesizes a detection of an object

without ever looking at it. The concept is explained in Fig. 1. The setup is a simple Mach–Zehnder interferometer, with 50/50 beam splitters BS1 and BS2, and two detectors D1 and D2. The arms of the interferometer are set in a way that the beam (of electrons or photons) interferes constructively on the detector D1 and destructively on detector D2. If an opaque object is entirely inserted in one of the two arms, there will be a 1/4 chance that the detector D2 will detect a photon (or an electron). In this way, the object can be detected without ever interacting with it.

The apparent limitation of this approach is that the efficiency of the measurements would be at most 50%.³⁰ This limit can be overcome by the repeated interrogation of the region and properly adjusting the reflectivity of the beam splitter.³² One possible implementation of this principle is shown in Fig. 1(c). Horizontally polarized photon is injected into the ring resonator with a waveplate and an interferometer. After the waveplate, the polarization cube reflects the vertical polarization into the object arm (dashed line). If no object is present, after N circulations, the polarization would be rotated to vertical and remain horizontal on the contrary case. In this set-up, the absorbed dose is proportional to the inverse of the number of interrogations. The key for understanding this apparent paradox is to note that the total dose (or probability of photon absorption) after N interrogations is the sum of the square of the wave function amplitude $\sum_1^N \frac{1}{N^2}$, while the probability of the photon detection in either case is the square of the sum of the wave function amplitude $(\sum_1^N \frac{1}{N})^2$. Alternatively, this can be thought of as a variation of the discrete Quantum Zeno effect, where sufficiently frequent interrogation of the system prevents it from decaying.³³ The efficiency above 50% was observed for optical systems, proving the viability of the concept.³¹ These concepts were successfully applied for dose-reduced imaging³⁴ and suggested for quantum cryptography.³⁵

It is conceptually plausible that a similar approach can be realized for electron microscopy, giving an invaluable tool for dose-dependent

measurements and single electron counting experiments.³⁶ Despite technical limitations, this and similar concepts³⁷ are currently in development, and their feasibility will be tested in the coming years. Besides interaction-free measurements, other quantum imaging techniques in optics will find their analogs in electron microscopy, such as quantum ghost imaging,³⁸ quantum illumination,³⁹ or delayed-choice measurements.⁴⁰

The described approach for low-dose imaging applications is based on real-space interference effects and requires no modification of the phase profile of the free-electron wave function. Other quantum phenomena in electron microscopy involve the active engineering of an electron's wave function employing phase plates or laser-based modulators. We first consider a longitudinal-phase modulation, which has already been proven useful for condensed matter applications.^{41–46} For observing quantum effects, such modulations have to be faster than the electron coherence time and thus faster than few tens of femtoseconds.⁴³ For this reason, such schemes are only implemented via the use of high-intensity ultrafast laser sources. Several recent experimental works have demonstrated that laser pulses can indeed modulate the longitudinal phase of an electron wave packet. Such a process can be viewed more intuitively in the energy domain as a coherent emission and absorption of photons by the electrons,^{41–44,47,48} similar to Rabi oscillations on a quantum ladder having infinite levels (Fig. 2).

This method brings several capabilities to electron microscopy. One phenomenon is the dispersive reshaping of the electron density into trains of attosecond pulses that can be used for attosecond electron microscopy and diffraction.^{43,48–53} Another is a quantum holography method based on the coherent interaction of the electron with multiple laser pulses.⁴⁹ This was recently implemented in our laboratory and applied to the dynamical observation of a nanoconfined electromagnetic field.⁴⁶

The fundamental principle of this holographic approach lies in the possibility of using light to modulate the phase of an electron wave

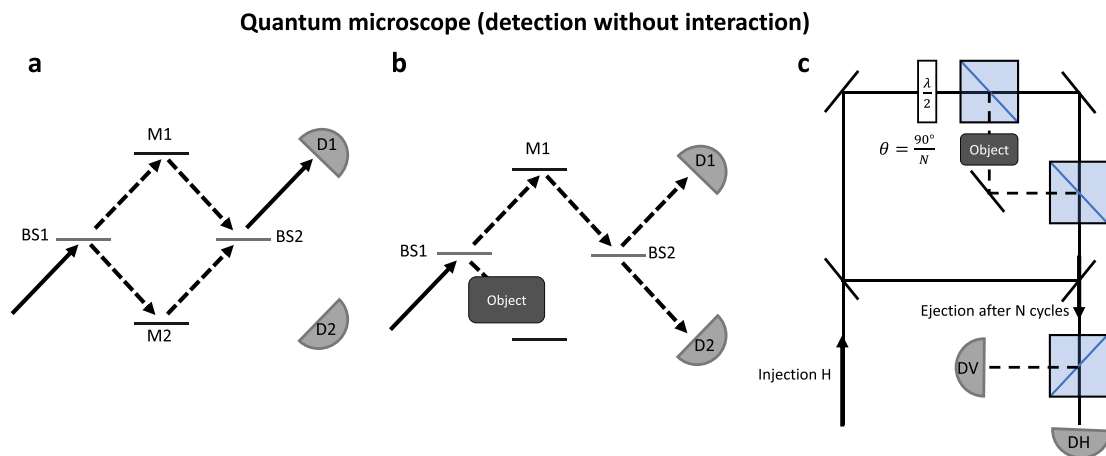


FIG. 1. Elitzur–Vaidman experiment as a basis for interaction-free measurements. (a) A device without an object. Mach–Zehnder interferometer is adjusted in a way that the incident wave (electron or photon) makes a constructive interference pattern on detector D1 and destructive interference pattern on detector D2. (b) The device with an object. The object is opaque. The photon goes to Mirror M1 with a 50% probability, and thus detector D2 has a 25% probability of detecting the presence of the object. (c) A setup for multiple interrogations of the object suggested in Ref. 31. The optical pulse is injected in the ring resonator from the bottom left corner. The waveplate rotates the polarization at each pass, with polarizing cube sending $1/N^2$ of intensity into Objects arm. If no object is present, the polarization rotates to Vertical after N rounds. In contrast, if the Object is present, the polarization will remain Horizontal.

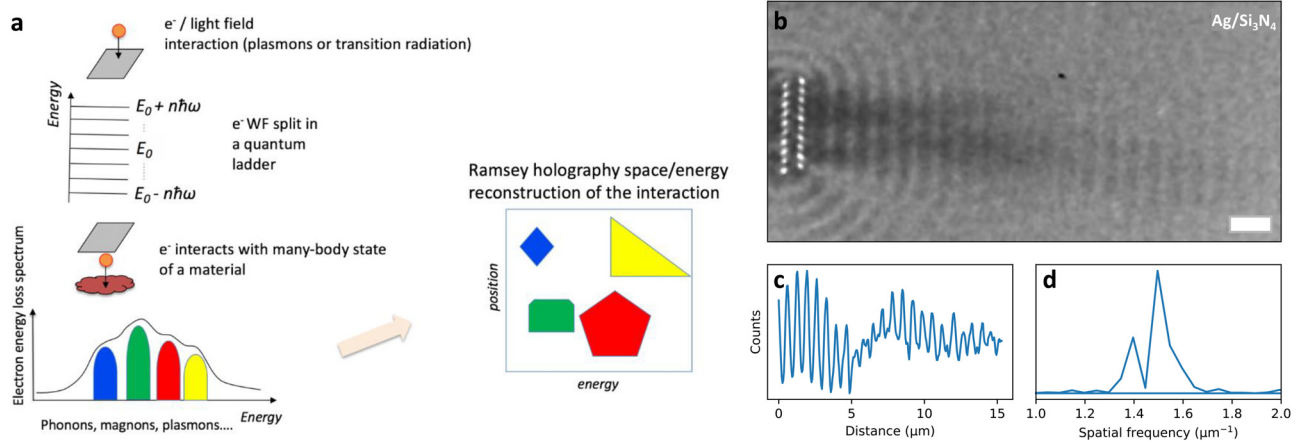


FIG. 2. (a) Principle of Ramsey holography applied to the spectroscopy of many-body states in solids: the different modes involved in a many-body state responsible for the inelastic interaction with the electrons will manipulate the electron wave function according to their spatial and temporal evolution, redistributing the electron wave function in energy and space. Such a modulation can be detected in the imaging plane of a transmission electron microscopy via energy-filtered electron microscopy (EFTEM), retrieving information on the different states and their mutual coherence at once. (b) An example of a holographic image of plasmon polaritons excited in the Ag/Si₃N₄ planar structure (scale bar 2 μm). (c) The vertically integrated intensity of the region of interest in panel (b), showing characteristic beatings (background removed). (d) Fourier transform of (c), showing two polariton modes corresponding to polaritons on Ag/Si₃N₄ and Ag/vacuum interfaces.

function. Indeed, since the optical profile can be directly imprinted onto the electron phase profile, the modulation by two optical pulses add up coherently. That is, if the two pulses are of the same amplitude and are in the antiphase, the modulation can even be canceled. Since a longitudinal modulation is associated with an energy splitting, one can judge the relative phase and amplitudes of two optical pulses by measuring the velocity distribution spectrum of the electrons.

In Fig. 2, we present a schematic of this technique in a TEM and its potential application to condensed matter spectroscopy. First, an electron pulse is made to interact with a spatially homogeneous reference field—a laser pulse reflected from an electron-transparent light-mirror.⁴³ This first interaction modulates the longitudinal phase of the electron and, therefore, its energy spectrum. The second optical pulse excites various modes in the material (phonons, excitons, plasmons, etc.). The interaction of the phase-shaped electron with these modes will re-modulate the phase of the electrons further. Thus, such additional modulations will be reflected in a variation of the electron energy spectrum after the specimen. By scanning through the phase-shift between the two pulses, the wave function can be entirely reconstructed, yielding information about the amplitude and the phase of the interaction to be tested.⁴⁸

The laser and the excitation fields can overlap in space, but, in general, they can be entirely spatially separated. For example, in Figs. 2(b)–2(d), we study two plasmon polariton modes existing on the opposite sides of the silver film at the interfaces with vacuum and dielectric substrate Si₃N₄, respectively. While the first plasmon interferes with the reference field in real space, the second is well screened by a 50 nm Ag film. A more intuitive way for understanding this holographic method is to view the reference and signal beams split in time instead of space. Electrons serve as a propagating phase-sensitive “photographic plate,” encountering first with the reference field and then with the unknown signal to be measured.

Besides the longitudinal phase modulation, also the transverse electron phase profile can be efficiently structured. This can be

performed either using static phase plates,^{54,55} laser cavity phase plates,¹⁹ or laser-induced nano-structured polariton modes.⁵³ Specifically, in our laboratory, we have demonstrated that a helical phase distribution can be imprinted on the electron wave packet by employing chiral plasmons carrying orbital angular momentum (OAM), thus generating an ultrafast vortex electron beam.⁵³ Due to the high degree of tunability of the driving optical field, the prominent feature of our approach is the ability to dynamically control the vortex beam structure on the attosecond time scale. Such a vortex dynamic control can allow for investigating nanoscale ultrafast processes in which chirality plays a significant role. Chirality is a crucial quantum concept in modern physics, especially in the context of topological materials whose properties are defined by spin–orbit coupling, time-reversal, crystalline, and particle–hole symmetries. As theoretically envisioned by Haldane,⁵⁶ the breaking of one or several of these symmetries prompts a substantial modification of the electronic structure and a radical change of the underlying order. As such, intriguing chiral phenomena can be directly imaged using the holographic approach described above when adopting ultrafast vortex electrons.

For example, time-reversal symmetry can be broken by photoexcitation with circularly polarized light, forming photon-dressed bands (Floquet bands).⁵⁷ When a pair of dressed bands hybridizes, each acquiring a non-trivial winding number, new protected edge modes can appear. For instance, edge plasmon polaritons can form in two branches with different velocities propagating along the opposite directions. Thus, a new class of collective electron modes with a chiral symmetry (Berry plasmons) could emerge.^{58,59} These types of processes would be particularly relevant in 3D magnetic semiconductors, where the magnetically controlled Berry curvature could be able to modify the propagation direction of such surface plasmons, creating a direct link between spintronic and plasmonic properties. Another class of materials with strong chiral properties is hexagonal materials with broken space-inversion symmetry where chiral phonons⁶⁰ have been

predicted as a possible handle for controlling inter-valley scattering in valleytronics applications.⁶¹

The selectivity of chiral interactions involving OAM electrons can be used not only for imaging applications but also to trigger or enhance chiral processes. An intriguing example for energy applications is the recently observed process of nuclear excitation by electron capture (NEEC).⁶² NEEC is a resonant process in which the capture of a free electron by an ion results in the resonant excitation of a nucleus, provided that the kinetic energy of the electron, E_k , equals the difference between the nuclear transition energy, E_n , and the atomic binding energy of the capture orbital, E_b (i.e., $E_k = E_n - E_b$). Besides energy, also the angular momentum must be conserved in the process. In particular, the total angular momentum change between the free and the captured electron states must match the nuclear spin variation. Thus, by providing electrons with a well-defined angular momentum, one would be able to choose the particular subset of orbitals in which they are captured, thus maximizing the efficiency of nuclear excitation per incident electron.

Further improvement in the efficiency of NEEC detection can be achieved in a variant of the process called NEECX,^{63,64} depicted in the top part of Fig. 3. Here, the capture does not occur in the electronic ground state but rather in an excited orbital. Because of this, the internal conversion (IC) channel of nuclear deexcitation is partially blocked, and deexcitation with gamma emission is more probable. Furthermore, such excited decay channels are characterized by a wider transition width compared to decay channels with fully occupied ground state [Fig. 3(d)]. The transition width can increase from few μeV to few meV, better matching the natural width of external electron sources. For example, in the case of a bare ^{238}U nucleus, the capture in the $2p_{1/2}$ subshell exhibits an integrated NEECX cross section, S_{NEECX} , about three orders of magnitude larger than the one for a non-excited atom.⁶³

Although electron microscopy applications inspired the concepts discussed above, these concepts are generally applicable to beams of

other massive composite particles in a variety of domains. In particular, for advanced microscopy, helium (He) ion microscopes and pumped atom lasers are two recent technologies that hold interest. The He ion microscopes discovered in 2006⁶⁵ can be beneficial to scanning electron microscopes (SEMs). In having a shorter de Broglie wavelength (tens of femtometers), He ion beams in the SEM can be focused to sub-nm probe sizes and provide a much-improved resolution on the ångström level. The stronger interaction with the sample means that femtoampere ion beam currents can be used, mitigating sample charging and, in some instances, beam-induced damage that occurs with electrons.^{65,66} As such, He ion microscopes have had the most impact on the fields of soft matter and biomaterial imaging. However, the proliferation of these microscopes to other research fields has been limited due to cost–benefit reasons. As with conventional electron microscopes, He ion guns can be made into pulsed sources for ultrafast experiments, and similar advantages for imaging and resolution can be gained by using pulsed He ions as a probe. The larger interaction cross sections may also mean that lower numbers of ions per pulse are required, reducing space–charge effects and providing a possible path to very high time resolution measurements.

Besides microscopy applications, engineering the wave function of composite particles has been recently shown to provide insight into sub-atomic phenomena. For instance, OAM-carrying neutrons would exhibit a modified internal charge distribution that, in a scattering experiment, could provide crucial insights into their internal arrangement of quarks and gluons.^{67,68} Similarly, we have predicted that vortex proton beams would exhibit an OAM-dependent density distribution, which will reflect its spin-dependent intrinsic properties⁵³ and may shed light on one of the long-standing open questions in sub-atomic physics: the origin of the proton spin.

The wave function reshaping methods described above could also be extended to atomic nuclei with intriguing consequences. Kammer *et al.* have considered a compelling case,⁶⁹ where they have calculated that wave function engineering can extend the lifetime of decaying particles, such as an unstable hydrogen isotope, or altering other decay processes. In practical applications, a composite particle wave function can be efficiently patterned via properly designed phase plates.^{70–72} When imparting orbital angular momentum to an atom or an ion,^{73,74} the inner charges/masses can redistribute in a doughnut shape, similar to what happens in the case of neutrons⁶⁷ and protons.⁵³ The effect of such mass redistribution can be included in the theory commonly used to describe nuclear excitations, the so-called liquid drop model.⁷⁵ In this framework, the nucleus is considered as a liquid drop whose excitations are its characteristic deformation modes, also called phonons in an analogy to structural vibrations in condensed matter. The spectrum of these “vibrations” and their shape determines the path and probability of the different decay processes. An axially deformed Woods–Saxon potential is used for energy level calculations.⁷⁶ Here, we solve the Schrödinger equation in spherical symmetry,⁷⁷ considering a modified Woods–Saxon potential that increases at the center of the nucleus and allows us to mimic mass redistribution (see the top panel in Fig. 4). The attractive potential leads to a significant renormalization of the energy levels for both protons and neutrons. In Fig. 4, we show the modified potential and the relative proton single particle energy states in the case of a double magic nucleus. It is instructive to note that different levels shift in a non-uniform way, potentially leading to a situation in which two close-lying nuclear

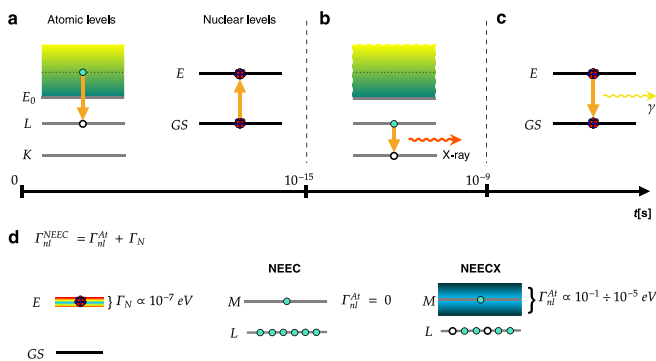


FIG. 3. In top panels, the nuclear excitation by the electron capture followed by a fast X-ray emission is depicted. In (a), the electron capture in the L shell induces a nuclear excitation (E), followed by an electron decay in the K shell with the emission of an X-ray photon after few femtoseconds (b). In (c), the nucleus slowly decays through a gamma-ray emission to the ground state (GS), since IC is blocked. Panel (d) describes how the presence of vacancies in lower shells, with respect to the one where capture occurs, leads to an increase in the transition width for NEECX. In NEEC, the electron capture leads only to the production of a nuclear-excited state, while for NEECX, it leads to double (atomic and nuclear) excited states.

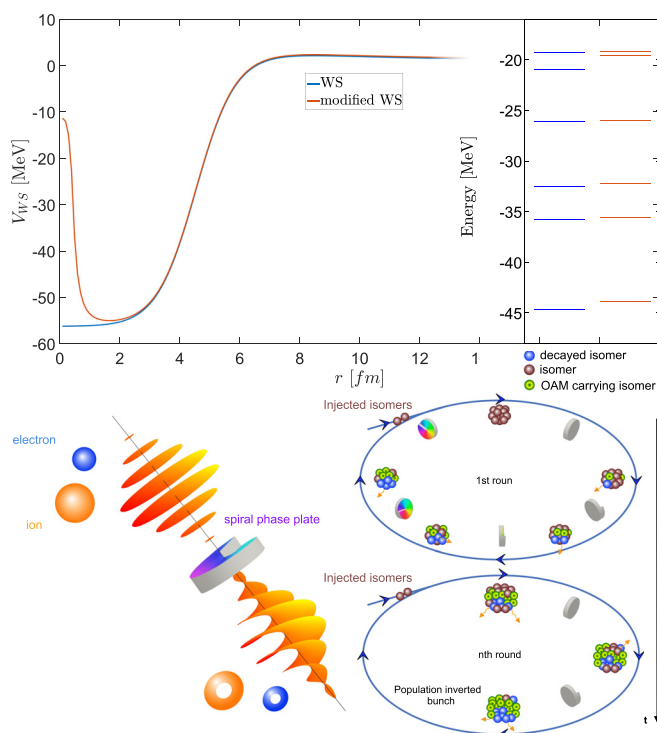


FIG. 4. (Top) Proton energy levels as calculated using a spherical Woods–Saxon potential. In the upper panel, a deformed potential is introduced to replicate the modulation induced by the vortex. (Bottom left) Phase vortex modulation could be imprinted on any de Broglie particle, as an electron (blue sphere) or an atom (orange sphere), by a spiral phase plate (SPP). Here, the curved arrows and the toroid symbolize that the particle is characterized by a defined orbital angular momentum, as well as a particular amplitude distribution (i.e., Laguerre–Gaussian). (Bottom right) Gamma-ray laser prototype where isomers are injected in a storage ring. SPPs are distributed along the path in order to induce a vortex modulation periodically.

levels would switch in energy between each other. An interesting example is ^{93}Mo , which could exhibit up to 10 orders of magnitude faster decay if the $21/2+$ and $17/2+$ spin states are reversed.⁷⁸

The possibility to manipulate decay rates of nuclei via phase modulation has far-reaching implications. For example, they can offer new solutions for gamma-ray lasers, for which historically, it has been challenging to reach the population inversion regime necessary to amplify a seed beam.⁷⁹ Various proposals and patents have been put forward using isomers, i.e., long-lived excited nuclei, as an active medium to provide gamma-rays. Still, only a few well-selected cases of isomers offered some perspective for reaching the population inversion regime. Here, we propose that the ability to modify at will a nuclear decay rate might be used for reaching population inversion in a stream of isomers. A schematic of such a concept is depicted in Fig. 4, lower panel. A beam of isomers is injected in a storage ring in which a device to impart OAM is placed periodically. Upon crossing such a device, a portion of the isomers will acquire OAM, while others will continue the circulation, and some will decay to their ground state through the usual channels. At the next OAM device, more isomers acquire OAM and so on for the remaining OAM devices. New isomers

are injected in the ring at a given rate. As more isomers acquire OAM, their decay rate can slow down until the point where the presence of excited isomers overcomes the inherent losses of the storage ring and the low probability of direct excitation by the gamma-rays emitted by the decaying isomers. In such a scenario, population inversion could happen and yield a net amplification of a seed gamma-ray beam. As discussed before, if switching between the two high-spin states of ^{93}Mo is possible, a subsequent fast depletion of the population can be triggered even without the necessity of a seed. The initial coherence required for the successful operation of the phase shaping devices can be provided by isomeric atomic lasers, which have already been considered as candidates for gamma-ray lasers.^{80,81} For the previously considered schemes, we believe that the wave function reshaping methods recently developed in the field of ultrafast electron microscopy will be an enabling technology for solving some of the long-standing issues behind these technologies.

To conclude, the utilization of quantum methods in electron microscopy based on interference effects and phase-manipulation of an electron wave function will lead to many new directions that have the potential of becoming independent research fields. The dose reduction approaches would be beneficial in biological applications, whereas wave function engineering approaches have clear benefits for condensed matter problems. At the same time, these tools and approaches can be applied as well to other matter-waves associated with composite particles, bringing potentially revolutionizing technologies for high-energy physics and energy domains.

AUTHORS' CONTRIBUTIONS

I.M. and G.M.V. contributed equally to this work.

The LUMES laboratory acknowledges support from the NCCR MUST, ERC Consolidator Grant; and Google Inc. G.M.V. is partially supported by the EPFL-MSCA international fellowship (Grant Agreement No. 665667). The authors would like to thank Dr. Alessandro Pastore, Dr. Roberto Tricarico, and Dr. Ido Kaminer for their helpful discussions.

REFERENCES

- ¹L. Reimer, *Transmission Electron Microscope: Physics Image Formation and Microanalysis* (Springer Berlin Heidelberg, Berlin, Heidelberg, 1984).
- ²D. Rossouw, M. Couillard, J. Vickery, E. Kumacheva, and G. A. Botton, *Nano Lett.* **11**, 1499 (2011).
- ³S. J. Pennycook, in *Scanning Transmission Electron Microscopy Imaging Analysis*, edited by S. J. Pennycook and P. D. Nellist (Springer, New York, 2011).
- ⁴R. Henderson, J. M. Baldwin, T. A. Ceska, F. Zemlin, E. Beckmann, and K. H. Downing, *J. Mol. Biol.* **213**, 899 (1990).
- ⁵N. Grigorieff, T. A. Ceska, K. H. Downing, J. M. Baldwin, and R. Henderson, *J. Mol. Biol.* **259**, 393 (1996).
- ⁶J. Frank, *Nat. Protoc.* **12**, 209 (2017).
- ⁷R. Fernandez-Leiro and S. H. W. Scheres, *Nature* **537**, 339 (2016).
- ⁸J. Dubochet, *Jacques Dubochet-Nobel Lecture in Chemistry* (World Scientific Publishing Co. Pte Ltd., 2017).
- ⁹A. H. Zewail and J. M. Thomas, *World Scientific, 4D Electron Microscopy: Imaging in Space and Time* (Imperial College Press, 2010).
- ¹⁰A. W. P. Fitzpatrick, U. J. Lorenz, G. M. Vanacore, and A. H. Zewail, *J. Am. Chem. Soc.* **135**, 19123 (2013).
- ¹¹A. W. P. Fitzpatrick, G. M. Vanacore, and A. H. Zewail, *Proc. Natl. Acad. Sci. U. S. A.* **112**, 3380 (2015).

- ¹²D. R. Cremons, D. A. Plemmons, and D. J. Flannigan, *Nat. Commun.* **7**, 11230 (2016).
- ¹³S. Sun, L. Wei, Z. Li, G. Cao, Y. Liu, W. J. Lu, Y. P. Sun, H. Tian, H. Yang, and J. Li, *Phys. Rev. B* **92**, 224303 (2015).
- ¹⁴G. Berruto, I. Madan, Y. Murooka, G. M. Vanacore, E. Pomarico, J. Rajeswari, R. Lamb, P. Huang, A. J. Kruchkov, Y. Togawa, T. LaGrange, D. McGrouther, H. M. Rønnow, and F. Carbone, *Phys. Rev. Lett.* **120**, 117201 (2018).
- ¹⁵L. A. Baker and J. L. Rubinstein, *Methods Enzymol.* **481**, 371 (2010).
- ¹⁶H. N. Chapman, P. Fromme, A. Barty, T. A. White, R. A. Kirian, A. Aquila, M. S. Hunter, J. Schulz, D. P. DePonte, U. Weierstall *et al.*, *Nature* **470**, 73 (2011).
- ¹⁷D. Cesar, J. Maxson, P. Musumeci, Y. Sun, J. Harrison, P. Frigola, F. H. O'Shea, H. To, D. Alesini, and R. K. Li, *Phys. Rev. Lett.* **117**, 024801 (2016).
- ¹⁸J. N. Longchamp, S. Rauschenbach, S. Abb, C. Escher, T. Latychevskaia, K. Kern, and H. W. Fink, *Proc. Natl. Acad. Sci. U. S. A.* **114**, 1474 (2017).
- ¹⁹O. Schwartz, J. J. Axelrod, S. L. Campbell, C. Turnbaugh, R. M. Glaeser, and H. Müller, *Nat. Methods* **16**, 1016 (2019).
- ²⁰G. McMullan, A. R. Faruqi, D. Clare, and R. Henderson, *Ultramicroscopy* **147**, 156 (2014).
- ²¹R. M. Glaeser, *Annu. Rev. Biophys.* **48**, 45 (2019).
- ²²H. W. Wang and X. Fan, *Curr. Opin. Struct. Biol.* **58**, 175 (2019).
- ²³M. Schorb, I. Haberbosch, W. J. H. Hagen, Y. Schwab, and D. N. Mastrorade, *Nat. Methods* **16**, 471 (2019).
- ²⁴J. Zivanov, T. Nakane, B. O. Forsberg, D. Kimanius, W. J. H. Hagen, E. Lindahl, and S. H. W. Scheres, *eLife* **7**, e42166 (2018).
- ²⁵M. Hohn, G. Tang, G. Goodyear, P. R. Baldwin, Z. Huang, P. A. Penczek, C. Yang, R. M. Glaeser, P. D. Adams, and S. J. Ludtke, *J. Struct. Biol.* **157**, 47 (2007).
- ²⁶See https://En.Wikibooks.Org/Wiki/Software_Tools_For_Molecular_Microscopy for “computational tools for molecular imaging.”
- ²⁷W. P. Putnam and M. F. Yanik, *Phys. Rev. A* **80**, 040902 (2009).
- ²⁸H. Okamoto, *Phys. Rev. A* **85**, 043810 (2012).
- ²⁹J. Steeds, P. G. Merli, G. Pozzi, G. Missiroli, and A. Tonomura, *Phys. World* **16**, 20 (2003).
- ³⁰A. C. Elitzur and L. Vaidman, *Found. Phys.* **23**, 987 (1993).
- ³¹P. G. Kwiat, A. G. White, J. R. Mitchell, O. Nairz, G. Weihs, H. Weinfurter, and A. Zeilinger, *Phys. Rev. Lett.* **83**, 4725 (1999).
- ³²P. Kwiat, H. Weinfurter, T. Herzog, A. Zeilinger, and M. A. Kasevich, *Phys. Rev. Lett.* **74**, 4763 (1995).
- ³³L. Vaidman, *Found. Phys.* **33**, 491 (2003).
- ³⁴A. G. White, J. R. Mitchell, O. Nairz, and P. G. Kwiat, *Phys. Rev. A* **58**, 605 (1998).
- ³⁵O. Hosten, M. T. Rakher, J. T. Barreiro, N. A. Peters, and P. G. Kwiat, *Nature* **439**, 949 (2006).
- ³⁶P. Kruit, R. G. Hobbs, C. S. Kim, Y. Yang, V. R. Manfrinato, J. Hammer, S. Thomas, P. Weber, B. Klopfer, C. Kohstall, T. Juffmann, M. A. Kasevich, P. Hommelhoff, and K. K. Berggren, *Ultramicroscopy* **164**, 31 (2016).
- ³⁷T. Juffmann, S. A. Koppell, B. B. Klopfer, C. Ophus, R. M. Glaeser, and M. A. Kasevich, *Sci. Rep.* **7**, 1699 (2017).
- ³⁸D. V. Strekalov, A. V. Sergienko, D. N. Klyshko, and Y. H. Shih, *Phys. Rev. Lett.* **74**, 3600 (1995).
- ³⁹S. Lloyd, *Science* **321**, 1463 (2008).
- ⁴⁰Y.-H. Kim, R. Yu, S. P. Kulik, Y. Shih, and M. O. Scully, *Phys. Rev. Lett.* **84**, 1 (2000).
- ⁴¹B. Barwick, D. J. Flannigan, and A. H. Zewail, *Nature* **462**, 902 (2009).
- ⁴²S. T. Park, M. Lin, and A. H. Zewail, *New J. Phys.* **12**, 123028 (2010).
- ⁴³G. M. Vanacore, I. Madan, G. Berruto, K. Wang, E. Pomarico, R. J. Lamb, D. McGrouther, I. Kaminer, B. Barwick, F. J. García de Abajo, and F. Carbone, *Nat. Commun.* **9**, 2694 (2018).
- ⁴⁴K. Wang, R. Dahan, M. Shentcis, Y. Kauffmann, S. Tsesses, and I. Kaminer, *arXiv:1908.06206* (2019).
- ⁴⁵O. Kfir, *Phys. Rev. Lett.* **123**, 103602 (2019).
- ⁴⁶I. Madan, G. M. Vanacore, E. Pomarico, G. Berruto, R. J. Lamb, D. McGrouther, T. T. A. Lummén, T. Latychevskaia, F. J. García de Abajo, and F. Carbone, *Sci. Adv.* **5**, eaav8358 (2019).
- ⁴⁷O. Kfir, H. Lourenço-Martins, G. Storeck, M. Sivis, T. R. Harvey, T. J. Kippenberg, A. Feist, and C. Ropers, *Nature* **582**, 46 (2020).
- ⁴⁸K. E. Priebe, C. Rathje, S. V. Yalunin, T. Hohage, A. Feist, S. Schäfer, and C. Ropers, *Nat. Photonics* **11**, 793 (2017).
- ⁴⁹K. E. Echternkamp, A. Feist, S. Schäfer, and C. Ropers, *Nat. Phys.* **12**, 1000 (2016).
- ⁵⁰Y. Morimoto and P. Baum, *Nat. Phys.* **14**, 252 (2018).
- ⁵¹M. Kozák, T. Eckstein, N. Schönerberger, and P. Hommelhoff, *Nat. Phys.* **14**, 121 (2018).
- ⁵²A. Feist, K. E. Echternkamp, J. Schauss, S. V. Yalunin, S. Schäfer, and C. Ropers, *Nature* **521**, 200 (2015).
- ⁵³G. M. Vanacore, G. Berruto, I. Madan, E. Pomarico, P. Biagioni, R. J. Lamb, D. McGrouther, O. Reinhardt, I. Kaminer, B. Barwick, H. Larocque, V. Grillo, E. Karimi, F. J. García de Abajo, and F. Carbone, *Nat. Mater.* **18**, 573 (2019).
- ⁵⁴J. Verbeeck, H. Tian, and P. Schattschneider, *Nature* **467**, 301 (2010).
- ⁵⁵V. Grillo, E. Karimi, G. C. Gazzadi, S. Frabboni, M. R. Dennis, and R. W. Boyd, *Phys. Rev. X* **4**, 011013 (2014).
- ⁵⁶F. D. M. Haldane, *Phys. Rev. Lett.* **61**, 2015 (1988).
- ⁵⁷Y. H. Wang, H. Steinberg, P. Jarillo-Herrero, and N. Gedik, *Science* **342**, 453 (2013).
- ⁵⁸T. Low, A. Chaves, J. D. Caldwell, A. Kumar, N. X. Fang, P. Avouris, T. F. Heinz, F. Guinea, L. Martin-Moreno, and F. Koppens, *Nat. Mater.* **16**, 182 (2017).
- ⁵⁹J. C. W. Song and M. S. Rudner, *Proc. Natl. Acad. Sci. U. S. A.* **113**, 4658 (2016).
- ⁶⁰H. Zhu, J. Yi, M.-Y. Li, J. Xiao, L. Zhang, C.-W. Yang, R. A. Kaindl, L.-J. Li, Y. Wang, and X. Zhang, *Science* **359**, 579 (2018).
- ⁶¹J. R. Schaibley, H. Yu, G. Clark, P. Rivera, J. S. Ross, K. L. Seyler, W. Yao, and X. Xu, *Nat. Rev. Mater.* **1**, 16055 (2016).
- ⁶²C. J. Chiara, J. J. Carroll, M. P. Carpenter, J. P. Greene, D. J. Hartley, R. V. F. Janssens, G. J. Lane, J. C. Marsh, D. A. Matterns, M. Polasik, J. Rzakiewicz, D. Seweryniak, S. Zhu, S. Bottoni, A. B. Hayes, and S. A. Karamian, *Nature* **554**, 216 (2018).
- ⁶³A. Pálffy, Z. Harman, C. Kozuharov, C. Brandau, C. H. Keitel, W. Scheid, and T. Stöhlker, *Phys. Lett. B* **661**, 330 (2008).
- ⁶⁴M. Polasik, K. Ślabkowska, J. J. Carroll, C. J. Chiara, Ł. Syrocki, E. We, derwe, der, and J. Rzakiewicz, *Phys. Rev. C* **95**, 34312 (2017).
- ⁶⁵J. Notte, B. Ward, N. Economou, R. Hill, R. Percival, L. Farkas, and S. McVey, *AIP Conf. Proc.* **931**, 489 (2007).
- ⁶⁶M. S. Joens, C. Huynh, J. M. Kasuboski, D. Ferranti, Y. J. Sigal, F. Zeitvogel, M. Obst, C. J. Burkhardt, K. P. Curran, S. H. Chalasani, L. A. Stern, B. Goetze, and J. A. J. Fitzpatrick, *Sci. Rep.* **3**, 3514 (2013).
- ⁶⁷H. Larocque, I. Kaminer, V. Grillo, R. W. Boyd, and E. Karimi, *Nat. Phys.* **14**, 1 (2018).
- ⁶⁸C. W. Clark, R. Barankov, M. G. Huber, M. Arif, D. G. Cory, and D. A. Pushin, *Nature* **525**, 504 (2015).
- ⁶⁹I. Kaminer, J. Nemirovsky, M. Rechtsman, R. Bekenstein, and M. Segev, *Nat. Phys.* **11**, 261 (2015).
- ⁷⁰A. D. Cronin, J. Schmiedmayer, and D. E. Pritchard, *Rev. Mod. Phys.* **81**, 1051 (2009).
- ⁷¹O. Carnal and J. Mlynek, *Phys. Rev. Lett.* **66**, 2689 (1991).
- ⁷²J. Fujita, M. Morinaga, T. Kishimoto, M. Yasuda, S. Matsui, and F. Shimizu, *Nature* **380**, 691 (1996).
- ⁷³V. E. Lembessis, D. Ellinas, M. Babiker, and O. Al-Dossary, *Phys. Rev. A* **89**, 53616 (2014).
- ⁷⁴V. E. Lembessis, *Phys. Rev. A* **96**, 13622 (2017).
- ⁷⁵A. Gagyí-Pálffy, *Theory of Nuclear Excitation by Electron Capture for Heavy Ions* (Justus-Liebig-Universität, 2006).
- ⁷⁶F. García, E. Garrote, M.-L. Yoneama, J. D. T. Arruda-Neto, J. Mesa, F. Bringas, J. F. Dias, V. P. Likhachev, O. Rodriguez, and F. Guzmán, *Eur. Phys. J. A* **6**, 49 (1999).
- ⁷⁷A. Pastore, see <https://sites.google.com/a/york.ac.uk/uknpss2019/programme/tutorial-projects/theory-tutorial> for “the numerical code used in the nuclear structure calculation.”
- ⁷⁸M. Hasegawa, Y. Sun, S. Tazaki, K. Kaneko, and T. Mizusaki, *Phys. Lett., Sect. B* **696**, 197 (2011).
- ⁷⁹F. J. Agee, *Hyperfine Interact.* **143**, 1 (2002).
- ⁸⁰G. R. Hoy, U.S. patent 7,425,706 (2008).
- ⁸¹L. J. Piekenbrock and E. Camp Tibbals, U.S. patent 3,557,370 (1971).